EurJIC
European Journal of Inorganic Chemistry

Full Papers
doi.org/10.1002/ejic.202100184

Chemistry Europe
European Chemical Societies Publishing

Synthesis, Staructure and Redox Properties of Cu(II) Chelate Complexes on the Basis of 2-(Hydroxyphenyl)-1H-benzo[d] imidazol-1-yl Phenol Ligands

Eugeny P. Ivakhnenko,*[a] Pavel A. Knyazev,[a] Yulia G. Vitkovskaya,[a] Leonid D. Popov,[b] Konstantin A. Lyssenko,[c] Oleg P. Demidov,[d] Andrey G. Starikov,[a] Gennady S. Borodkin,[a] and Vladimir I. Minkin[a]

A series of 2-(hydroxyphenyl)-1H-benzo[d]imidazols bearing readily oxidizable 2,6-di-tert-butyl-phenol substituents and bis-chelate Cu(II) complexes based on these ligands were synthesized. The structure of the compounds was characterized by NMR, IR, mass spectroscopy and X-ray crystallographic analysis and redox behavior explored using ESR spectra and cyclic voltammetry. Under oxidation with PbO_2 in toluene solution both the ligands and Cu(II) complexes form stable phenoxyl-type radicals. As shown by ESR measurements and DFT calculations, no exchange interaction exists between unpaired electrons located on metal and oxygen centers in the biradical Cu (II) complexes. The ligands and complexes reveal antioxidant radical scavenging activity measured spectrophotometrically and using ESR and DPPH-tests.

Introduction

Metal complexes with ligands functionalized with readily oxidizable 2,6-di-*tert*-butylphenol moieties have drawn significant interest as active antioxidants, antiphlogistic specimens, radioprotectors and absorbers of various reactive oxygen species (ROS).[1–4] The central metal ions of such type coordination compounds, especially those having unpaired electrons as Cu(II) ions, contribute to the production of phenoxyl radicals and substantially modify their stability and reactivity.[1,5,6] Copper is an essential element responsible for the function of many cellular enzymes, such as cytochrome **c** oxidase, NADH dehydrogenase 2, tyrosinases and proteins.[7,8] The previous studies[9,10] revealed particularly high antioxidant and antiaggregant properties of benzimidazole derivatives containing spatially hindered phenol moieties efficiently inhibiting oxidative stress. Metal coordination changes the redox potential and additionally affects its antioxidant capacity.[11] Therefore, the goals of the present work consisted in the synthesis, structural characterization of Cu(II) complexes with the 2,6-di-*tert*-butylphenol-containing ligands and comparative study of redox activity and stability of the corresponding phenoxyl radicals formed in the oxidation. As the appropriate ligands bearing 2,6-di-*tert*-butylphenol pendants we have chosen 2,6-di-*tert*-butyl-4-(2-(2-hydroxyphenyl)-1H-benzo[d]imidazol-1-yl)phenols **3** known to exhibit pronounced antioxidant and antiplatelet activities.[9,10] The compounds were synthesized in good yields by the reaction of quinone imines **1** with various derivatives of salicylic aldehyde (Scheme 1) in general accordance with the

[a] *Prof. Dr. E. P. Ivakhnenko, P. A. Knyazev, Y. G. Vitkovskaya, Dr. A. G. Starikov, G. S. Borodkin, Prof. Dr. V. I. Minkin*
Institute of Physical and Organic Chemistry
Southern Federal University
194/2 Stachki st., Rostov-on-Don,
344090, Russian Federation
E-mail: ivakhnenko@sfedu.ru
https://twitter.com/sfedu_official
[b] *L. D. Popov*
Chemistry Department
Southern Federal University
7 Zorge st., Rostov-on-Don,
344090, Russian Federation
[c] *Dr. K. A. Lyssenko*
A.N. Nesmeyanov Institute of Organoelement Compounds
Russian Academy of Sciences
28 Vavilov st., Moscow,
119991, Russian Federation
[d] *Dr. O. P. Demidov*
North Caucasus Federal University
1 Pushkin st., Stavropol,
355017, Russian Federation

Supporting information for this article is available on the WWW under https://doi.org/10.1002/ejic.202100184

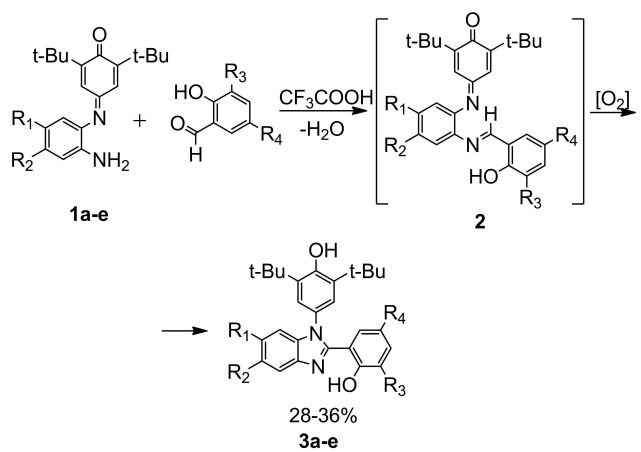

Scheme 1. Synthesis of 1-(3,5-di-tert-butyl-4-hydroxyphenyl)-2-hydroxyarylbenzimidazoles **3** (**a**-$R_1=R_2=R_3=R_4=H$; **b**-$R_1=R_2=H$; $R_3=R_4=$t-Bu; **c**-$R_1=R_2=CH_3$; $R_3=R_4=H$; **d**-$R_2=OCH_3$; $R_1=R_3=R_4=H$; **e**-$R_1=COOC_2H_5$; $R_2=R_3=R_4=H$).

procedures described for some of the previously obtained compounds of this group.[12–17]

The structures of the newly prepared compounds (**1b**–**e**, **3b**–**e**) were established on the basis of the data of IR-, mass- and ^{1}H NMR spectroscopy and elemental analyses. The compounds are stable in their enol OH forms **3**. The DFT B3LYP-6/311++G(d,p) calculation with the account taken for solvation (toluene) showed that the keto NH form of the parent hydroxyphenylbenzimidazol **3a** is energy disfavored by 3.3 kcal/mol. Molecular and structure of this compound featuring its enol form was determined using X-ray crystallography and shown in Figure 1.

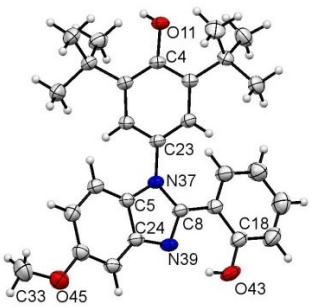

Figure 1. The shape of a molecule of 2,6-di-*tert*-butyl-4-(2-(2-hydroxyphenyl)-5-methoxy-1H-benzo[d]imidazol-1-yl)phenol **3d**. Selected bond lengths (Å): C4–O11 1.3677(15), N37–C5 1.3930(18), N37–C8 1.3786(17), N37–C23 1.4401(15), N39–C8 1.3301(17), N39–C24 1.3766(19), C18–O43 1.347(2). The dihedral angle (rotation about the C23–N37 axis is equal to 57.05°.

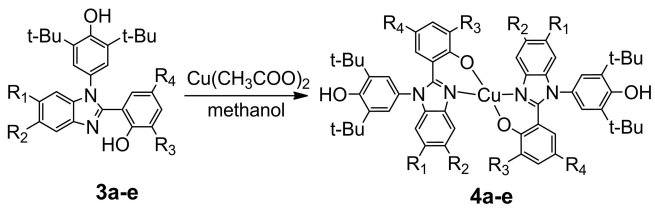

Scheme 2. Synthesis of bis-chelate Cu(II) complexes of 1-(3,5-di-tert-butyl-4-hydroxyphenyl)-2-hydroxyarylbenzimidazole ligands.

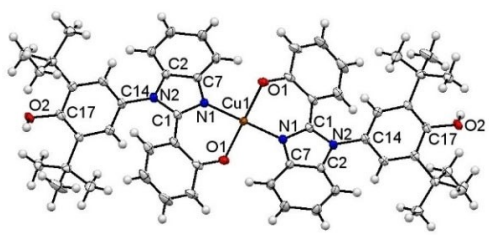

Figure 2. View of the molecular structure of complex **4a**. The dihedral angle (rotation about the C14–N2 bond is equal to 60.59°. Selected bond lengths (Å): Cu1–O1 1.9212(11), Cu1–N1 1.9652(12), C17–O2 1.386(2).

Results and Discussion

Synthesis and structures of Cu(II) complexes

Reaction of 2,6-di-*tert*-butyl-4-(2-(2-hydroxyphenyl)-1H-benzo[d]imidazol-1-yl)phenols **3** with Cu(II) acetate readily occurs at short-term reflux of the methanol solutions of the components to give well crystallized bis-chelate complexes **4** in good or moderate yields (Scheme 2). Molecular structures of two prepared complexes were determined using X-ray crystallography and are pictured in Figure 2 and Figure 3.

In complexes 4, the central Cu(II) ions four-coordinated to two N atoms and two O atoms from benzimidazole ligands adopt planar, slightly tetrahedrally distorted configuration. The two Cu–N, as well as the Cu–O bond lengths, are nearly equivalent. The 3,5-di-tert-butylphenol rings are diverted from the plane of the rest of the molecules by the angles about 60° which sharply reduces their π-conjugation with the core of the molecule and restrict delocalization of unpaired electron of the phenoxyl radicals produced from the complexes.

The B3LYP-6311++G(d,p) computed structure of **4a** (Figure 9) found at the doublet potential energy surface also reveals chair-like distortion of the bis-chelate coordination site and well reproduces the experimental geometry (Figure 2).

Central Cu(II) ion of complexes **4** is coordinatively unsaturated and readily form additional bonds with electron donor centers of external agents. Thus, solution of **4a** in chloroform leads to the formation of a six-coordinated Cu(II) adduct **4a**·$(CHCl_3)_2$. Stability of this adduct caused by the Cu···Cl binding contacts agrees with the recent findings indicating that transition metal complexes can act as halogen bond acceptors.[18,19] Solution of **4a** in dimethylsulfoxide also affords a stable pentacoordinated Cu(II) adduct **4a**·DMSO. The XRD molecular structures of these compounds are shown in Figure 4 and Figure 5.

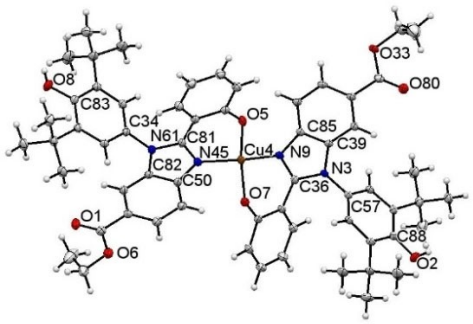

Figure 3. View of the molecular structure of complex **4e**. The dihedral angles (rotation about the C34–N61 and C57–N3 bonds are equal to 65.76° and 50.51°, respectfully. Selected bond lengths (Å): Cu4–O5 1.8880(16), Cu1–O7 1.8990(16), Cu4–N9 2.0138(17), Cu4–N45 1.9669(16), C88–O2 1.361(3), C83–O8 1.363(2).

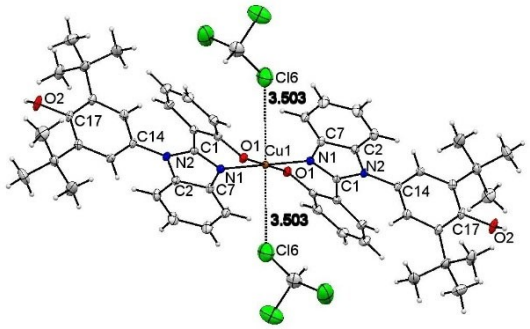

Figure 4. View of the molecular structure of complex **4 a**·$(CHCl_3)_2$. The dihedral angle (rotation about the C14–N2 bond is equal to 86.91°. Selected bond lengths (Å): Cu1–O1 1.9212(11), Cu1–N1 1.9652(12), C17–O2 1.386(2).

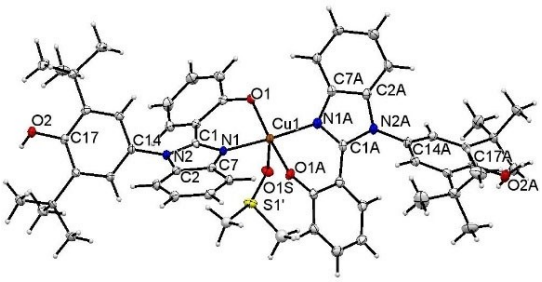

Figure 5. View of the molecular structure of complex **4 a**·DMSO. The dihedral angles (rotation about the C14–N2 and C14A–N2A bonds are equal to 59.11° and 57.07°, respectfully. Selected bond lengths (Å): Cu1–O1 1.925(2), Cu1–O1A 1.945(2), Cu1–N1 1.984(3), Cu1–N1A 1.999(3), Cu1–O1S 2.285(2), O2–C17 1.369(4), O2A–C17A 1.375(4).

Free radicals

Antioxidative properties of α-tocopherol related to scavenging secondary radicals are determined by the formation of α-tocopheroxyl radical,[4,20] which led to intense studies of various synthetic analogues-precursors of phenoxyl radicals. In this direction, significant attention was given to antioxidant activities of benzimidazol derivatives of sterically crowded phenols.[2,3,6,15] We have found that oxidation of hydroxyphenylbenzimidazoles **3** with PbO_2 in toluene or chloroform solutions readily affords phenoxyl radicals stable at room temperature in the absence of dioxygen for at least 5–7 days (Scheme 3). ESR spectrum of phenoxyl radical **5 a** shown in Figure 6 demonstrates coupling of the unpaired electron with two equivalent meta-protons of the phenoxyl ring and imine nitrogen atom (^{14}N, S = 1). Spectral parameters of this and other observed stable radicals **5** are listed in Table 1. It is worth of noting that isotropic g-values and spin coupling constants remain practically equal for all studied radicals, which is explained by the diversion of the unpaired electron containing moieties from the common plane and cutting off their conjugation with the benzimidazole π-system (see Figures 2–4).

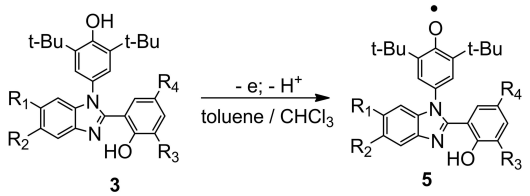

Scheme 3. Formation of phenoxyl radicals **5** by oxidation of **3** with PbO_2 in toluene or chloroform solutions.

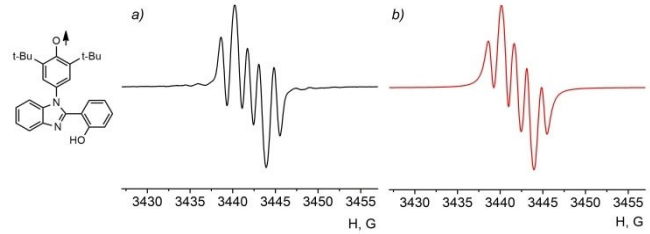

Figure 6. Experimental (a) and calculated (b) spectra of radical **5 a** (toluene, 300 K).

ESR spectra of complex **4 a** are shown in Figure 7. It contains four hyperfine structure lines indicated coupling the unpaired electron with the copper nucleus (S = 3/2). The more intense highest-field line features additional hyperfine structure caused by coupling the unpaired electron of copper with two equivalent paramagnetic ^{14}N nuclei (S = 1) (Figure 7, red). Addition of PbO_2 to a toluene solution of **4 a** leads to oxidation of a phenol hydroxyl group to produce the triradical **6**. The ESR spectrum of **6** shown in Figure 8 represent superposition of signals of non-interacting unpaired electrons related to Cu(II)

Table 1. ESR spectral parameters of phenoxyl radicals **5**.

Radical	a^N	$a^H_{3,5}$	g	Solvent
5 a	1.30	1.78	2.005	Toluene
5 b	1.56	1.70	2.005	Toluene
5 c	1.22	1.70	2.004	Chloroform
5 d	1.30	1.73	2.005	Chloroform
5 e	1.32	1.82	2.005	Chloroform

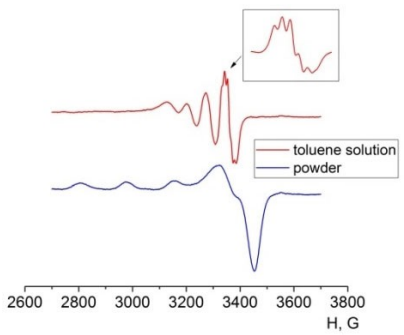

Figure 7. ESR spectrum of Cu(II) complex **4 a** in toluene solution (red): a^{Cu} = 70.8 G; $a^N_{1,2}$ = 10.7 G; g = 2.12 and of a powder sample (blue): a^{Cu} = 172.8 G; g = 2.27).

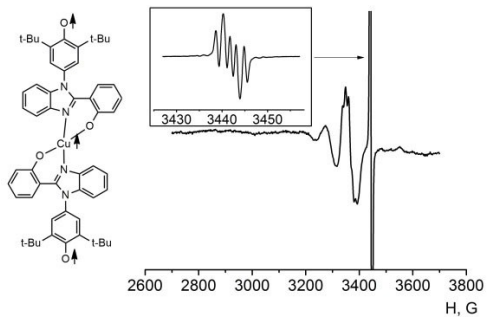

Figure 8. ESR spectrum of triradical **6** obtained by oxidation of complex **4a** in toluene solution with excess PbO_2 ($a^{Cu}=70.8$ G; $a^{N}_{1,2}=10.7$ G; g = 2.12; *incut*-$a^{N}=1.30$ G; $a^{H}_{3,5}=1.78$ G; g = 2.005).

ion ($a^{Cu}=70.8$ G; $a^{N}_{1,2}=10.7$ G; g = 2.12) and free phenoxyl radical (g = 2.005; $a^{N}=1.30$ G; $a^{H}_{3,5}=1.78$ G). The ESR spectra for complexes **4b**–**e** are identical to the spectra of complex **4a**.

Geometries and spin distributions of complex **4a**, biradical **6a** and triradical **6** calculated with the use of DFT B3LYP-6311 + + G(d,p) are shown in Figure 9.

In accordance with experimental data (Figure 7, Figure 8) the calculations showed that in spite of the conjugate π-electron systems of all the species, no exchange interactions exist between the unpaired electrons located at metal and phenoxyl oxygen centers. Spin coupling values J_{CuO} and J_{OO} calculated based on the broken symmetry approach[21,22] are negligible (in the range 0–0.02 cm^{-1}).

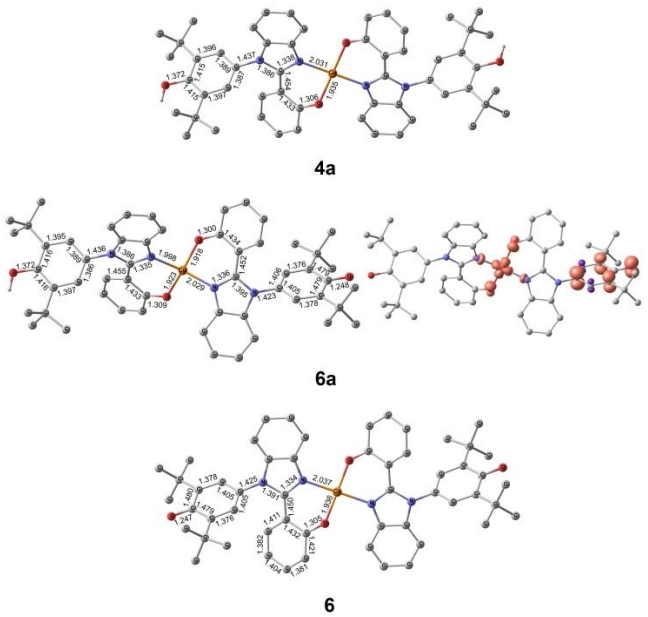

Figure 9. Optimized geometries and spin distribution in complex **4a** and radicals generated by its oxidation calculated by the DFT (B3LYP/6-311 + + G(d,p) method. Spin density distribution in biradical **6a** is shown on the right. Bond lengths are given in Angstroms, hydrogen atoms with the exception of hydroxy groups are omitted for clarity.

Cyclic voltammetry

Electrochemical properties of complexes **4a**, **4b** and their ligands **3a** and **3b** were studied using cyclic voltammetry of dichloromethane solutions (Figure 10).

Redox behavior of the complexes is characterized by two irreversible oxidation waves, the first of which is caused by oxidation of one of two hydroxy group with the potentials $E_{1/2}{}^{1}=0.34$ V (**4a**) and $E_{1/2}{}^{1}=0.37$ B (**4b**) and the second one with the potentials $E_{1/2}{}^{2}=0.56$ B (**4a**) and $E_{1/2}{}^{2}=0.60$ B (**4b**) is, most likely, associated with oxidation of the second hydroxy group. Parameters of the CV collected in Table 2 clearly evidence significantly lower values of the potentials of oxidation of phenol hydroxyl groups of Cu(II) complexes as compared with those characteristic of their free ligands.

Scavenging activity

The ability of 2-(hydroxyphenyl)-1H-benzo[d]imidazols and their Cu(II) complexes to readily produce highly stable phenoxyl-type radicals provide for the antioxidant properties of these compounds. Their scavenging activity was tested using the standard procedure involving the reaction of hydrogen atom transfer to the stable free radical 2,2-diphenyl-1-picrylhydrazyl (DPPH).[11,23,24] The reaction can be spectrophotometrically monitored by measuring decrease in absorption of the intense longest wavelength band ($I_{max}=517$ nm, ethanol) of DPPH (Figure S29–S32). The degree of the reduction of DPPH ("radical inhibition") was calculated according to the formula:[25]

$$Q = 100 \cdot (A_0\text{-}A_c)/A_0$$

where A_0 is the initial absorbance and A_c is the value for added sample concentration *c*.

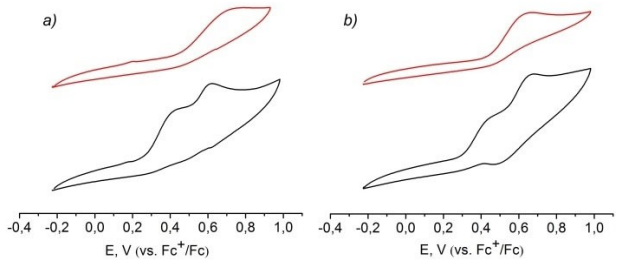

Figure 10. Cyclic voltammograms of **a)** oxidation of ligand **3a** (red) and Cu(II) complex **4a** (black) and **b**) of ligand **3b** (red) and complex **4b** (black).

Table 2. CV parameters of compounds **3a**, **3b**, **4a** and **4b**.

Compound	$E_{1/2}{}^{1}$, [V]	$E_{1/2}{}^{2}$, [V]
3a	0.58	
4a	0.34	0.56
3b	0.54	
4b	0.37	0.60

For the reaction of phenol **3a** with DPPH proceeding at 290 K for 1 hour the value $Q_{290} = 13.7\%$, whereas at 348 K (Figure S29) the value Q_{348} increases to 37.8% and the calculated time needed to consume 50% of the initial DPPH concentration $\tau\ (50)_{348} = 154.6$ min (Figure S30). For a Cu(II) complex **4a** the corresponding values of Q and τ are the following: $Q_{290} = 8.4\%$; $Q_{348K} = 19.3\%$; $\tau\ (50)_{348} = 168.1$ min. Development of the reactions between the hydroxyphenyl-containing ligands and Cu(II) complexes with DPPH was traced by evolution of their ESR spectra. Figure 11 demonstrates superposition of signals produced by DPPH ($g_{DPPH} = 2.00$, $a^{2N}_{DPPH} = 8.94$ G) and the phenoxyl radical **5a** ($g_{5a} = 2.00$, $a^{N} = 1.30$ G, $a^{2H} = 1.78$ G formed through abstraction of a hydrogen atom from **3a**. Intensity of the first signal is gradually degraded with time (few minutes), while that of the second one is synchronously extinguished.

Conclusion

To sum up, we have synthesized and determined molecular structures of a series of novel chelate ligands, 2-hydroxyphenyl-1H-benzo[d]imidazols functionalized with readily oxidizable 2,6-di-*tert*-butyl-phenol substituents. Two bis-chelate Cu(II) complexes based on these ligands and two their stable crystal solvates were structurally characterized by X-ray crystallography. Chemical oxidation of the ligands and complexes with 2,6-di-*tert*-butylphenol pendant fragments studied by means of ESR method reveals the formation of highly stable phenoxyl type radicals, particularly stable in the case of biradicals produced by the Cu(II) complexes. This feature, as well as the substantially lower values of the potentials of oxidation of phenol hydroxyl groups of Cu(II) complexes as compared with those of their free ligands (Table 2, Figure 10) witness enhanced antioxidative properties of metal complexes **4** inherent in promising scavengers for ROSs. This finding provides an additional support to the earlier observations of positive effects rendered by metal ions and metal binding sites on the antioxidant activity of organic radical scavengers.[6,7,26]

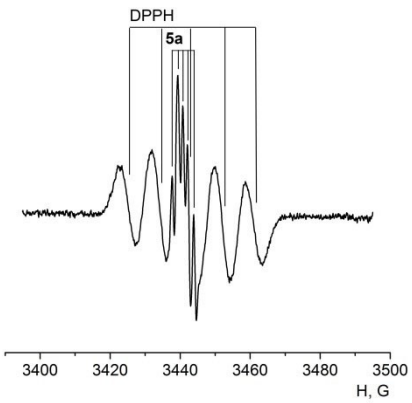

Figure 11. ESR spectrum featuring the formation of radical **5a** (peaks appearing in the central part of the spectrum) upon interaction of **3a** with DPPH (toluene, T = 290 K, $g_{DPPH} = 2.00$, $a^{2N}_{DPPH} = 8.94$ G; $g_{5a} = 2.00$, $a^{N} = 1.30$ G, $a^{2H} = 1.78$ G).

Experimental Section

Materials and methods

All reagents and solvents were purchased from commercial sources (Aldrich) and used without additional purification. The compounds were characterized by ^{1}H and ^{13}C NMR, IR-, mass spectra and elemental analysis. ^{1}H NMR spectra were recorded on Varian (300 MHz) spectrometers in $CDCl_3$ solutions. The signals were referred with regard to the signals of residual protons of deutero-solvents (7.24 ppm), δ values were measured with precision 0.01 ppm. Elemental analysis was performed by the classical micro-analysis method. High-resolution mass spectra were recorded on a Bruker maXis Impact UHR-TOF mass spectrometer (electrospray ionization). Melting points were determined using a PTP (M) apparatus and were left uncorrected. Control on the progress of the reactions and the individuality of products of the reactions was accomplished using thin layer chromatography with Silufol UV-245 wafers (benzene and methylene dichloride as eluents and iodine as developer). IR spectra were recorded on a Varian Excalibur 3100 FT-IR instrument using the attenuated total internal reflection technique (ZnSe crystal). ESR measurements were carried out on X-band spectrometer Bruker EMX Plus. The theoretical spectrum was calculated using the Bruker WinEPR Simfonia v.1.25 program. The cyclic voltammograms of benzimidazoles **3a,b** and their complexes **4a,b** were measured in 5 mM solution with the use of three-electrode configuration (glassy-carbon working electrode, Pt counter electrode, Ag/Ag^{+} reference electrode (0.01 M $AgNO_3$ in CH_3CN)) and potentiostat–galvanostat Elins P-45X. The ferrocene/ferrocenium (Fc/Fc^{+}) couple served as internal reference. Electronic absorption spectra were recorded on a Varian Cary 5000 instrument in the range of 400–700 nm. The dynamic DPPH test measured the optical density of a solution with the same concentration of antioxidant and DPPH radicals. Several measurements were made of the same solution at regular intervals. Then a graph was plotted as the percentage of absorbed radicals versus time. The constant τ (50), the time required for the absorption of 50% DPPH radicals, was determined from the graph.

The datasets of reflections from single crystals were obtained on an automated diffractometer Bruker SMART APEX II CCD diffractometer [λ(MoKα) = 0.71072 Å, ω-scans] (complex **4a**) and on an Agilent SuperNova diffractometer using microfocus X-ray source (complex **4e**) and Atlas S2 CCD detector. The collection of reflexes, determination and refinement of unit cell parameters were performed with the aid of the specialized CrysAlisPro 1.171.38.41 software suite.[27] The structures were solved by using ShelXT program,[28] structure refinement was also performed with the ShelXL program.[29] Positions of hydrogen atoms were calculated geometrically and included in the refinement as riding groups. Molecular graphics were rendered and prepared for publication with the Olex2 software suite.[30] Selected crystal data of compounds **3d**, **4a** and **4e** are given in Supporting Information. The complete X-ray diffraction datasets were deposited at the Cambridge Crystallographic Data Center.

The density functional theory calculations were performed using the Gaussian 16 program package[31] with the UB3LYP hybrid functional[32] and the 6-311++G(d,p) basis set including diffuse and polarization functions at all atoms. The stationary points on the potential energy surfaces (PESs) were located by full geometry optimization with calculation of force constant matrices indicating

the correspondence of the structures obtained to the minima on the PES and checked for the stabilities of DFT wave function. Exchange coupling of unpaired electrons in the paramagnetic centres was estimated using the "broken symmetry" (BS) approach.[21] The exchange coupling constants J (in cm^{-1}) were calculated with the use of generalized spin-projection method developed by Yamaguchi.[22] For the search of the BS states, the Gaussian 16 procedure (Guess = Fragment = N) has been employed. This technique implies a possibility to assume spin states and signs along with charges for separate parts of a molecule on the stage of generation of the initial guess. Structural visualizations presented in Figure 9 were prepared using the ChemCraft software[33] with the calculated atomic coordinates as input parameters.

Quinone imines

General procedures

Solution of 0.220 g (1.0 mmol) of 2,6-di-*tert*-butyl-*p*-benzoquinone, 1.0 mmol of the corresponding *o*-phenylenediamine and catalytic amounts of trifluoroacetic acid in 30 ml of toluene was refluxed for 4 hours with Dean-Stark attachment until the release of water stops. After cooling the reaction mixture was purified by column chromatography (carrier-Al_2O_3, eluent – toluene) to give the product.

4-(2-aminophenyl)imino)-2,6-di-tert-butylcyclohexa-2,5-dienone 1 a. Yield 80%. Physical and spectral data are identical to those described in [13]. **^{13}C NMR** (600 MHz, $CDCl_3$) δ: 29.48, 29.49 (*tert*-Bu: C–CH_3), 35.30, 35.76 (*tert*-Bu: C–CH_3); arom.: 115.57, 117.88, 121.41, 122.20, 128.11, 135.71 (C–N=), 134.94, 141.60 (C–NH_2); 152.33, 153.27 (C-*tert*-Bu); 157.60 (C=N–); 187.90 (C=O).

4-(2-amino-4,5-dimethylphenyl)imino)-2,6-di-tert-butylcyclohexa-2,5-dienone 1 b. Violet crystals. Yield 75%. M.p. 154–155 °C. **IR** (nujol, cm^{-1}): 3440 (w), 3344 (w), 2998 (w), 2954 (s), 2925 (s), 2855 (m), 1644 (m), 1626 (m), 1586 (w), 1560 (w), 1522 (w), 1493 (w), 1456 (w), 1413 (w), 1376 (w), 1361 (w), 1332 (w), 1311 (w), 1288 (w), 1268 (w), 1249 (w), 1221 (w), 1197 (w), 1168 (w), 1107 (w), 1075 (w), 1022 (w), 1003 (w), 938 (w), 887 (w), 886 (w), 863 (w), 822 (w), 733 (w), 671 (w), 570 (w). **^{1}H NMR** (300 MHz, $CDCl_3$) δ: 1.24 (s, 9H, *tert*-Bu); 1.32 (s, 9H, *tert*-Bu); 2.14 (s, 3H, CH_3); 2.20 (s, 3H, CH_3); 3.97 (s, 2H, NH_2); arom.: 6.44 (s, 1H), 6.61 (s, 1H); 7.04 (d, 1H, J = 2.5 Hz), 7.13 (d, 1H, J = 2.5 Hz). **^{13}C NMR** (600 MHz, $CDCl_3$) δ: 18.73 (CH_3), 19.69 (CH_3); 29.51, 29.53 (*tert*-Bu: C–CH_3), 35.25, 35.73 (*tert*-Bu: C–CH_3); arom.: 117.12, 122.51, 133.81 (C–N=), 140.12 (C–NH_2), 135.14; 137.30 (C–CH_3), 122.85 (C–CH_3); 151.77, 152.56 (C-*tert*-Bu); 156.54 (C=N–); 187.94 (C=O). **HRMS** (ESI) m/z: $[M+H]^+$ calcd for $C_{22}H_{31}N_2O$ 339.2431; found 339.2434. Anal. calcd. for $C_{22}H_{30}N_2O$: C, 78.06; H, 8.93; N, 8.28; found: C, 78.10; H, 8.91; N, 8.28.

4-((2-amino-5-methoxyphenyl)imino)-2,6-di-tert-butylcyclohexa-2,5-dienone 1 c. Violet crystals. Yield 43%. M.p. 72–73 °C. **IR** (nujol, cm^{-1}): 3468 (w), 3368 (w), 3317 (w), 2956 (s), 2921 (s), 2853 (s), 1614 (m), 1505 (w), 1485 (w), 1463 (m), 1455 (m), 1377 (w), 1362 (w), 1338 (w), 1312 (w), 1296 (m), 1261 (m), 1213 (w), 1170 (w), 1139 (w), 1078 (w), 1025 (w), 962 (w), 936 (w), 915 (w), 885 (w), 823 (w), 807 (w), 742 (w), 723 (w), 652 (w), 634 (w), 617 (w), 568 (w). **^{1}H NMR** (300 MHz, $CDCl_3$) δ: 1.25 (s, 9H, *tert*-Bu); 1.32 (s, 9H, *tert*-Bu); 3.79 (s, 3H, O–CH_3); 4.26 (s, 2H, NH_2); arom.: 6.29–6.34 (m, 2H), 6.60 (d, 1H, J = 8.6 Hz); 7.03 (d, 1H, J = 2.6 Hz), 7.12 (d, 1H, J = 2.6 Hz). **^{13}C NMR** (600 MHz, $CDCl_3$) δ: 29.52, 29.54 (*tert*-Bu: C–CH_3), 35.22, 35.72 (*tert*-Bu: C–CH_3); 55.34 (O–CH_3); arom.: 100.44, 104.03, 122.36, 123.09, 129.81 (C–N=), 135.22, 144.50 (C–NH_2); 151.40, 152.48 (C-*tert*-Bu); 155.50 (C=N–); 160.82 (C–OCH_3) 188.06 (C=O). **HRMS** (ESI) m/z: $[M+H]^+$ calcd for $C_{21}H_{29}N_2O_2$ 341.2224; found 341.2229. Anal. calcd. for $C_{21}H_{28}N_2O_2$: C, 74.08; H, 8.29; N, 8.23; found: C, 74.05; H, 8.30; N, 8.24.

Ethyl 4-amino-3-((3,5-di-tert-butyl-4-oxocyclohexa-2,5-dien-1-ylidene)amino)benzoate 1 d. Red crystals. Yield 55%. M.p. 177–178 °C. **IR** (nujol, cm^{-1}): 3466 (m), 3357 (m), 2954 (s), 2921 (s), 2854 (s), 1687 (s), 1662 (s), 1639 (w), 1621 (m), 1602 (m), 1581 (w), 1522 (w), 1498 (w), 1487 (w), 1456 (m), 1416 (w), 1390 (w), 1364 (m), 1345 (w), 1316 (m), 1294 (m), 1253 (m), 1223 (w), 1192 (w), 1155 (w), 1107 (w), 1082 (w), 1025 (w), 938 (w), 926 (w), 904 (w), 884 (w), 831 (w), 818 (w), 796 (w), 767 (w), 737 (w), 659 (w), 642 (w), 612 (w), 562 (w). **^{1}H NMR** (300 MHz, $CDCl_3$) δ: 1.23 (s, 9H, *tert*-Bu); 1.32 (s, 9H, *tert*-Bu); 1.32 (t, 3H, CH_3); 4.30 (q, 2H, CH_2); 4.49 (s, 2H, NH_2); arom.: 6.76 (d, 1H, J = 8.4 Hz), 7.04 (d, 1H, J = 2.5 Hz), 7.09 (d, 1H, J = 2.5 Hz), 7.36 (d, 1H, J = 1.9 Hz), 7.77 (dd, 1H, J = 8.4, 1.9 Hz). **^{13}C NMR** (600 MHz, $CDCl_3$) δ: 14.40 (O–CH_2–CH_3); 29.45, 29.48 (*tert*-Bu: C–CH_3), 35.35, 35.84 (*tert*-Bu: C–CH_3); 60.44 (O–CH_2–CH_3); arom.: 114.28, 119.57 (C–N=), 121.95, 123.14, 129.97, 134.15 (C–NH_2), 134.64, 146.01 (C–COOEt); 152.75, 153.59 (C-*tert*-Bu); 158.40 (C=N–); 166.39 (COOEt) 187.78 (C=O). **HRMS** (ESI) m/z: $[M+H]^+$ calcd for $C_{23}H_{31}N_2O_3$ 383.2329; found 383.2338. Anal. calcd. for $C_{23}H_{30}N_2O_3$: C, 72.22; H, 7.91; N, 7.32; found: C, 72.25; H, 7.90; N, 7.31.

4-((2-amino-5-nitrophenyl)imino)-2,6-di-tert-butylcyclohexa-2,5-dienone 1 e. Dark red crystals. Yield 69%. M.p. 182–183 °C. **IR** (nujol, cm^{-1}): 3450 (w), 3435 (w), 3348 (m), 3296 (w), 3184 (w), 3109 (w), 3070 (w), 2957 (s), 2925 (s), 2855 (m), 1650 (m), 1633 (m), 1614 (m), 1588 (w), 1569 (w), 1494 (w), 1463 (w), 1377 (w), 1364 (w), 1308 (m), 1267 (w), 1250 (w), 1197 (w), 1168 (w), 1151 (w), 1099 (w), 1080 (w), 1024 (w), 956 (w), 935 (w), 902 (w), 883 (w), 825 (w), 805 (w), 751 (w), 737 (w), 722 (w), 685 (w), 661 (w), 644 (w), 615 (w), 578 (w). **^{1}H NMR** (300 MHz, $CDCl_3$) δ: 1.23 (s, 9H, *tert*-Bu), 1.32 (s, 9H, *tert*-Bu); 4.76 (s, 2H, NH_2); arom.: 6.74 (d, 1H, J = 8.7 Hz), 7.01 (s, 2H), 7.59 (d, 1H, J = 2.7 Hz), 7.99 (dd, 1H, J^1 = 8.7 Hz, J^2 = 2.7 Hz). **^{13}C NMR** (600 MHz, $CDCl_3$) δ: 29.43, 29.45 (*tert*-Bu: C–CH_3), 35.45, 36.00 (*tert*-Bu: C–CH_3); arom.: 113.47, 116.89, 121.06, 124.10, 133.51 (C–N=), 134.21, 147.38 (C–NH_2); 138.56 (C–NO_2), 153.62, 154.86 (C-*tert*-Bu); 159.80 (C=N–); 187.45 (C=O). **HRMS** (ESI) m/z: $[M-H]^-$ calcd for $C_{20}H_{24}N_3O_3$ 354.1823; found 354.1822. Anal. calcd. for $C_{20}H_{25}N_3O_3$: C, 67.58; H, 7.09; N, 11.82; found: C, 67.60; H, 7.10; N, 11.81.

Benzo[d]imidazol-1-yl phenols. General procedure

A solution of a equimolar amounts (0.16–1.36 mmol) of *p*-quinone imine **1** and 2-hydroxy-3,5-di-(*tert*-butyl)benzaldehyde (compounds **3 b**) or salicylic aldehyde (compounds **3 a**, **c**–**e**) in toluene (5–30 mL) was stirred at the refluxing temperature for 3–8 h. (CF_3COOH was used as the catalyst). The reaction mixture was cooled to the room temperature and the formed deposit filtered off. The crude products were purified by column chromatography sorbent Al_2O_3, eluent toluene).

2,6-di-tert-butyl-4-(2-(2-hydroxyphenyl)-1H-benzo[d]imidazol-1-yl)phenol 3 a. Physical and spectra data is identical to those described in [13, 15]. **^{13}C NMR** (600 MHz, $CDCl_3$) δ: 30.17 (*tert*-Bu: C–CH_3), 34.62 (*tert*-Bu: C–CH_3); arom.: 110.59, 112.55, 117.64, 117.94, 118.56, 123.15, 123.48, 124.29, 127.24, 128.51, 131.25, 136.65, 138.04, 139.89; 150.94 (C=N–); 154.40 (C–OH), 159.76 (C–OH).

2,6-di-tert-butyl-4-(2-(3,5-di-tert-butyl-2-hydroxyphenyl)-1H-benzo[d]imidazol-1-yl)phenol 3 b. Yellowish crystals. Yield 35%. M.p. 226 °C. **IR** (nujol, cm^{-1}): 3624 (m), 2997 (w), 2956 (s), 2930 (s), 2854 (s), 1772 (w), 1618 (w), 1591 (w), 1559 (w), 1541 (w), 1518 (w), 1498 (w), 1468 (m), 1461 (m), 1441 (m), 1401 (w), 1391 (w), 1371 (w), 1361 (w), 1325 (w), 1313 (w), 1277 (m), 1261 (w), 1236 (m), 1202 (w), 1153 (w), 1117 (w), 1060 (w), 1026 (w), 1006 (w), 944 (w), 931 (w), 899 (w), 880 (w), 848 (w), 825 (w), 809 (w), 775 (w), 750 (w), 716 (w), 678 (w), 639 (w), 623 (w), 575 (w). **^{1}H NMR** (300 MHz, $CDCl_3$) δ: 0.97

(s, 9H, *tert*-Bu), 1.43 (s, 18H, *tert*-Bu), 1.49 (s, 9H, *tert*-Bu); 5.48 (s, 1H, OH); arom.: 6.98–7.77 (m, 8H); 14.04 (s, 1H, OH). **^{13}C NMR** (600 MHz, $CDCl_3$) δ: 29.60, 30.17, 31.26 (*tert*-Bu: C–CH_3), 33.94, 34.58, 35.37 (*tert*-Bu: C–CH_3); arom.: 110.51, 111.67, 118.26, 122.24, 122.91, 123.09, 124.52, 125.78, 129.55, 137.01, 137.27, 138.20, 138.75, 139.70; 152.21 (C=N–); 154.35 (C–OH), 156.48 (C–OH). **HRMS** (ESI) m/z: $[M-H]^-$ calcd for $C_{35}H_{45}N_2O_2$ 525.3487; found 525.3477. Anal. calcd. for $C_{35}H_{46}N_2O_2$: C, 79.81; H, 8.80; N, 5.32; found: C, 79.86; H, 8.82; N, 5.30.

2,6-di-tert-butyl-4-(2-(2-hydroxyphenyl)-5,6-dimethyl-1H-benzo [d]imidazol-1-yl)phenol 3c. White powder. Yield 36%. M.p. 227–229 °C. **IR** (nujol, cm^{-1}): 3632 (w), 3585 (w), 2954 (s), 2923 (s), 2854 (s), 1629 (w), 1587 (w), 1508 (w), 1486 (m), 1467 (m), 1440 (m), 1416 (w), 1378 (w), 1331 (w), 1298 (w), 1257 (w), 1238 (w), 1201 (w), 1172 (w), 1159 (w), 1119 (w), 1097 (w), 1035 (w), 999 (w), 948 (w), 903 (w), 853 (w), 824 (w), 758 (w), 723 (w), 683 (w), 658 (w), 618 (w), 577 (w). **^{1}H NMR** (300 MHz, $CDCl_3$) δ: 1.43 (s, 18H, *tert*-Bu); 2.34 (s, 3H, CH_3), 2.40 (s, 3H, CH_3); 5.49 (s, 1H, OH); arom.: 6.46–7.21 (m, 8H); 13.85 (s, 1H, OH). **^{13}C NMR** (600 MHz, $CDCl_3$) δ: 20.22 (CH_3), 20.55 (CH_3); 30.20 (*tert*-Bu: C–CH_3), 34.62 (*tert*-Bu: C–CH_3); arom.: 110.67, 112.85, 117.57, 117.88, 118.60, 124.34, 127.01, 128.75, 130.91, 132.20, 132.85, 135.16, 137.96; 150.12 (C=N–); 154.31 (C–OH), 159.60 (C–OH). **HRMS** (ESI) m/z: $[M-H]^-$ calcd for $C_{29}H_{33}N_2O_2$ 441.2548; found 441.2540. Anal. calcd. for $C_{29}H_{34}N_2O_2$: C, 78.70; H, 7.74; N, 6.33; found: C, 78.65; H, 7.74; N, 6.31.

2,6-di-tert-butyl-4-(2-(2-hydroxyphenyl)-5-methoxy-1H-benzo[d] imidazol-1-yl)phenol 3d. Light green crystals. Yield 28%. M.p. 193–195 °C. **IR** (nujol, cm^{-1}): 3543 (w), 3530 (w), 3090 (w), 3066 (w), 3039 (w), 2997 (w), 2953 (s), 2921 (s), 2855 (m), 1600 (m), 1541 (w), 1522 (w), 1504 (w), 1486 (m), 1463 (m), 1454 (m), 1440 (m), 1420 (m), 1389 (w), 1376 (w), 1352 (w), 1330 (w), 1293 (w), 1278 (w), 1266 (w), 1253 (w), 1237 (m), 1197 (w), 1167 (m), 1109 (m), 1038 (w), 955 (w), 934 (w), 916 (w), 888 (w), 843 (w), 819 (w), 791 (w), 779 (w), 742 (w), 695 (w), 656 (w), 639 (w), 624 (w), 577 (w). **^{1}H NMR** (300 MHz, $CDCl_3$) δ: 1.42 (s, 18H, *tert*-Bu); 3.89 (s, 3H, O–CH_3); 5.49 (s, 1H, OH); arom.: 6.48–7.26 (m, 9H); 13.73 (s, 1H, OH). **^{13}C NMR** (600 MHz, $CDCl_3$) δ: 30.18 (*tert*-Bu: C–CH_3), 34.62 (*tert*-Bu: C–CH_3); 55.95 (O–CH_3); arom.: 100.69, 111.01, 112.70, 113.62, 117.63, 117.91, 124.22, 127.04, 128.59, 131.09, 131.34, 138.00, 140.62; 150.96 (C=N–); 154.35 (C–OH); 156.97 (C–OCH_3); 159.61 (C–OH). **HRMS** (ESI) m/z: $[M-H]^-$ calcd for $C_{28}H_{31}N_2O_3$ 443.2340; found 443.2322. Anal. calcd. for $C_{28}H_{32}N_2O_3$: C, 75.65; H, 7.26; N, 6.30; found: C, 75.60; H, 7.27; N, 6.31.

Ethyl-1-(3,5-di-tert-butyl-4-hydroxyphenyl)-2-(2-hydroxyphenyl)-1H-benzo[d]imidazole-6-carboxylate 3e. White powder. Yield 28%. M.p. 208–209 °C. **IR** (nujol, cm^{-1}): 3572 (w), 3520 (m), 3393 (w), 3053 (w), 2956 (s), 2919 (s), 2854 (s), 1773 (w), 1706 (s), 1664 (w), 1612 (w), 1582 (w), 1559 (w), 1541 (w), 1505 (w), 1480 (m), 1455 (m), 1436 (m), 1411 (m), 1378 (w), 1367 (w), 1321 (w), 1292 (s), 1255 (m), 1238 (m), 1201 (w), 1158 (w), 1128 (m), 1116 (m), 1099 (m), 1028 (w), 962 (w), 942 (w), 929 (w), 915 (w), 888 (w), 845 (w), 833 (w), 810 (w), 773 (w), 749 (m), 699 (w), 672 (w), 654 (w), 631 (w), 616 (w), 577 (w). **^{1}H NMR** (300 MHz, $CDCl_3$) δ: 1.36–1.40 (m, 3H, CH_3); 1.43 (s, 18H, *tert*-Bu); 4.36 (q, 2H, CH_2, $J = 7.1$ Hz); 5.56 (s, 1H, OH); arom.: 6.50–8.05 (m, 9H); 13.57 (s, 1H, OH). **^{13}C NMR** (600 MHz, $CDCl_3$) δ: 14.35 (O–CH_2–CH_3); 30.15 (*tert*-Bu: C–CH_3), 34.65 (*tert*-Bu: C–CH_3); 61.02 (O–CH_2–CH_3); arom.: 112.09, 112.93, 117.84, 118.02, 118.16, 124.25, 124.61, 125.73, 127.46, 127.95, 131.95, 136.44, 138.25, 143.26 (C–COOEt); 153.37 (C=N–); 154.73 (C–OH), 160.03 (C–OH); 166.90 (COOEt). **HRMS** (ESI) m/z: $[M-H]^-$ calcd for $C_{30}H_{33}N_2O_4$ 485.2446; found 485.2431. Anal. calcd. for $C_{30}H_{34}N_2O_4$: C, 74.05; H, 7.04; N, 5.76; found: C, 74.09; H, 7.03; N, 5.75.

Cu(II) complexes

General procedure

Solution of a benzo[d]imidazol-1-yl-phenol **3** (0.1 mmol) in methanol (10 mL) was added with methanol solution (5 mL) of half equivalent amount (0.05 mmol) of monohydrate of $Cu(CH_3COO)_2$ and the common solution was heated to boiling for 1 h. The reaction mixture was cooled to the room temperature and allowed to stand for 6–10 h. The formed deposit filtered off and purified by crystallization from methanol.

Bis(2,6-di-tert-butyl-4-(2-(2-hydroxyphenyl)-1H-benzo[d]imidazol-1-yl)phenol) copper(II) 4a. Light green powder. Yield 35%. M.p. >330 °C. **IR** (nujol, cm^{-1}): 3624 (m), 3101 (w), 3060 (w), 2953 (s), 2924 (s), 2854 (s), 1603 (m), 1547 (m), 1498 (m), 1470 (s), 1435 (m), 1421 (m), 1377 (w), 1366 (w), 1338 (m), 1307 (w), 1292 (w), 1280 (w), 1263 (m), 1254 (m), 1232 (m), 1201 (w), 1151 (w), 1137 (w), 1117 (w), 1103 (w), 1031 (w), 1018 (w), 941 (w), 890 (w), 870 (w), 850 (w), 816 (w), 756 (w), 740 (m), 703 (w), 684 (w), 659 (w), 626 (w), 568 (w). Anal. Calc. for $C_{54}H_{58}CuN_4O_4$: C, 72.82; H, 6.56; N, 6.29; Found: C, 72.80; H, 6.48; N, 6.24.

Bis(2,6-di-tert-butyl-4-(2-(3,5-di-tert-butyl-2-hydroxyphenyl)-1H-benzo[d]imidazol-1-yl)phenol) copper(II) 4b. Brown-gray powder. Yield 74%. M.p. 238–240 °C. **IR** (nujol, cm^{-1}): 3670 (w), 3638 (m), 3585 (w), 2953 (s), 2920 (s), 2853 (s), 1614 (m), 1512 (m), 1469 (s), 1456 (m), 1441 (m), 1404 (w), 1378 (m), 1362 (w), 1335 (w), 1316 (m), 1293 (w), 1260 (m), 1238 (m), 1201 (w), 1154 (w), 1119 (w), 1066 (w), 1025 (w), 1010 (w), 953 (w), 932 (w), 903 (w), 885 (w), 868 (w), 834 (w), 815 (w), 791 (w), 759 (w), 748 (w), 726 (w), 692 (w), 638 (w), 616 (w), 569 (w). Anal. Calc. for $C_{70}H_{90}CuN_4O_4$: C, 75.40; H, 8.14; N, 5.02; Found: C, 75.46; H, 8.17; N, 5.05.

Bis(2,6-di-tert-butyl-4-(2-(2-hydroxyphenyl)-5,6-dimethyl-1H-benzo[d]imidazol-1-yl)phenol) copper(II) 4c. Brown powder. Yield 78%. M.p. >350 °C. **IR** (nujol, cm^{-1}): 3429 (w), 2955 (s), 2921 (s), 2853 (s), 1601 (w), 1556 (w), 1475 (m), 1466 (m), 1440 (m), 1403 (w), 1377 (w), 1338 (w), 1316 (w), 1253 (m), 1239 (m), 1201 (w), 1173 (w), 1160 (w), 1133 (w), 1122 (w), 1105 (w), 1036 (w), 1023 (w), 995 (w), 944 (w), 930 (w), 892 (w), 858 (w), 837 (w), 761 (w), 722 (w), 705 (w), 692 (w), 648 (w), 616 (w), 574 (w). Anal. Calc. for $C_{58}H_{66}CuN_4O_4$: C, 73.58; H, 7.03; N, 5.92; Found: C, 73.64; H, 7.00; N, 5.87.

Bis(2,6-di-tert-butyl-4-(2-(2-hydroxyphenyl)-5-methoxy-1H-benzo [d]imidazol-1-yl)phenol) copper(II) 4d. Dark green crystals. Yield 60%. M.p. >300 °C. **IR** (nujol, cm^{-1}): 3616 (w), 2954 (s), 2923 (s), 2855 (s), 1619 (w), 1599 (w), 1554 (w), 1470 (m), 1422 (w), 1377 (w), 1337 (w), 1316 (w), 1256 (w), 1237 (w), 1205 (w), 1153 (w), 1119 (w), 1105 (w), 1036 (w), 964 (w), 937 (w), 904 (w), 837 (w), 804 (w), 788 (w), 755 (w), 723 (w), 653 (w), 622 (w). Anal. Calc. for $C_{55}H_{59}CuN_4O_5$: C, 71.83; H, 6.47; N, 6.09; Found: C, 71.80; H, 6.42; N, 6.13.

Bis(ethyl-1-(3,5-di-tert-butyl-4-hydroxyphenyl)-2-(2-hydroxyphenyl)-1H-benzo[d]imidazole-6-carboxylate) copper(II) 4e. Dark green small rhombic crystals. Yield 70%. M.p. >350 °C. **IR** (nujol, cm^{-1}): 3581 (w), 2955 (s), 2923 (s), 2854 (s), 1749 (w), 1707 (m), 1616 (w), 1601 (w), 1548 (w), 1500 (w), 1470 (m), 1437 (w), 1420 (w), 1392 (w), 1376 (w), 1336 (w), 1317 (w), 1288 (w), 1271 (w), 1247 (m), 1208 (w), 1157 (w), 1130 (w), 1099 (w), 1030 (w), 965 (w), 935 (w), 892 (w), 865 (w), 851 (w), 824 (w), 774 (w), 754 (w), 727 (w), 678 (w), 652 (w), 639 (w), 577 (w). Anal. Calc. for $C_{60}H_{66}CuN_4O_8$: C, 69.65; H, 6.43; N, 5.41; Found: C, 69.71; H, 6.44; N, 5.50.

Deposition Numbers 2045191 (**3d**), 1838301 (**4a**), 1838303 (**4a**·$(CHCl_3)_2$), 1838309 (**4a**·DMSO), and 2045192 (**4e**) contain the supplementary crystallographic data for this paper. These data are provided free of charge by the joint Cambridge Crystallographic

Data Centre and Fachinformationszentrum Karlsruhe Access Structures service www.ccdc.cam.ac.uk/structures.

Acknowledgements

Research was financially supported by Ministry of Science and Higher Education of the Russian Federation (state assignment in the field of scientific activity, project 0852-2020-0031).

Conflict of Interest

The authors declare no conflict of interest.

Keywords: Cu(II) complexes · Phenoxyl radicals · Biradicals · Triradicals · DFT calculations

[1] H. Kozlowski, A. Janicka-Klos, J. Brasun, E. Gaggelli, D. Valensin, G. Valensin, *Coord. Chem. Rev.* **2009**, *253*, 2665–2685.
[2] E. R. Milaeva, S. I. Filimonova, N. N. Meleshonkova, L. G. Dubova, E. F. Shevtsova, S. O. Bachurin, N. S. Zefirov, *Bioinorg. Chem. Appl.* **2010**, *2010*, 165482.
[3] V. Yu Tyurin, J. Zhang, A. Glukhova, E. R. Milaeva, *Macroheterocycles* **2011**, *4*, 211–212.
[4] J. L. Bolton, T. Dunlap, *Chem. Res. Toxicol.* **2017**, *30*, 13–37.
[5] T. Jähnert, M. D. Hagerab, U. S. Schubert, *J. Mater. Chem. A* **2014**, *2*, 15234.
[6] E. R. Milaeva, D. B. Shpakovsky, Yu. A. Gracheva, S. I. Orlova, V. V. Maduar, B. N. Tarasevich, N. N. Meleshonkova, L. G. Dubova, E. F. Shevtsova, *Dalton Trans.* **2013**, *42*, 6817–6829.
[7] E. I. Solomon, D. E. Heppner, E. M. Johnston, J. W. Ginsbach, J. Cirera, M. Qayyum, M. T. Kieber-Emmons, C. H. Kjaergaard, R. G. Hadt, Li Tian, *Chem. Rev.* **2014**, *114*, 3659–3853.
[8] R. A. Festa, D. J. Thiele, *Curr. Biol.* **2011**, *21*, R877-R883.
[9] A. A. Spasov, A. F. Kucheryavenko, K. A. Gaidukova, V. A. Kosolapov, O. N. Zhukovskaya . *Res.Pharm.*. **2020**, *6*, 1–9.
[10] A. Baldiserotto, M. Demurtas, I. Lampronti, M. Tacchini, D. Moi, G. Balboni, S. Pacifico, S. Vertuani, S. Manfredini, V. Onnis, *Bioorg. Chem.* **2020**, *94*, 103396.
[11] L. Tabrisi, D. Quang Dao, T. An Vu, *RSC Adv.* **2019**, *9*, 3320–3335.
[12] K. Goto, K. Hashimoto, K. Kanai, *Jpn. KokaiTokkyoKoho* **1989**, JP 64000074A 19890105.
[13] V. N. Komissarov, *Chem. Heterocycl. Compd.* **1990**, *4*, 414–416.
[14] L. Yu, Ukhin, K. Y. Suponitskii, L. V. Belousova, T. N. Gribanova, *Russ. Chem. Bull.* **2009**, *58*, 940–943.
[15] T. O. Khubaeva, R. S. Zakaeva, *Russ. J. Gen. Chem.* **2012**, *82*, 446–454.
[16] T. O. Khubaeva, I. V. Khubaeva, *Russ. J. Gen. Chem.* **2013**, *83*, 1703–1706.
[17] A. V. Metelitsa, V. N. Komissarov, M. I. Knyazhansky, V. I. Minkin, *Mol. Cryst. Liq. Cryst.* **1997**, *297*, 219–226.
[18] D. M. Ivanov, A. S. Novikov, I. V. Ananyev, Y. V. Kirina, Y. V. Kukushkin, *Chem. Commun.* **2016**, *55*, 5565–5568.
[19] I. Alkorta, J. Elguero, A. Frontera, *Crystals* **2020**, *10*, 180.
[20] R. Yamauchi, *J. Clin. Biochem. Nutr.* **2004**, *34*, 111–120.
[21] L. Noodleman, *J. Chem. Phys.* **1981**, *74*, 5737–5743.
[22] M. Shoji, K. Koizumi, Y. Kitagawa, T. Kawakami, S. Yamanaka, M. Okumura, K. Yamaguchi, *Chem. Phys. Lett.* **2006**, *432*, 343–347.
[23] E. M. Becker, L. R. Nissen, L. H. Skibsted *Eur. Food Res. Technol.* **2004**, *219*, 561–571.
[24] M. S. Chernov'yants, T. S. Kolesnikova, A. O. Karginova, *Talanta.* **2016**, *149*, 319–325.
[25] P. Molyneux, *J. Sci. Technol.* **2004**, *26*, 2, 211–219.
[26] S. A. Cherrak, N. Mokhtari-Soulimane, F. Berroukeche, B. Bensenane, A. Cherbonnel, H. Merzouk, M. Elhabiri, *PLOS ONE* **2016**, *11*, e0165575.
[27] CrysAlisPro, version 1.171.38.41; Rigaku Oxford Diffraction, 2015. https://www.rigaku.com/en/products/smc/crysalis.
[28] G. M. Sheldrick, *Acta Crystallogr. Sect. A* **2008**, *64*, 112–122.
[29] G. M. Sheldrick, *Acta Crystallogr. Sect. C* **2015**, *71*, 3–8.
[30] O. V. Dolomanov, L. J. Bourhis, R. J. Gildea, J. A. K. Howard, H. Puschmann, *J. Appl. Crystallogr.* **2009**, *42*, 339–341.
[31] M. J. Frisch, G. W. Trucks, H. B. Schlegel, G. E. Scuseria, M. A. Robb, J. R. Cheeseman, G. Scalmani, V. Barone, B. Mennucci, G. A. Petersson, H. Nakatsuji, M. Caricato, X. Li, H. P. Hratchian, A. F. Izmaylov, J. Bloino, G. Zheng, J. L. Sonnenberg, M. Hada, M. Ehara, K. Toyota, R. Fukuda, J. Hasegawa, M. Ishida, T. Nakajima, Y. Honda, O. Kitao, H. Nakai, T. Vreven, J. A. Montgomery Jr., J. E. Peralta, F. Ogliaro, M. Bearpark, J. J. Heyd, E. Brothers, K. N. Kudin, V. N. Staroverov, T. Keith, R. Kobayashi, J. Normand, K. Raghavachari, A. Rendell, J. C. Burant, S. S. Iyengar, J. Tomasi, M. Cossi, N. Rega, J. M. Millam, M. Klene, J. E. Knox, J. B. Cross, V. Bakken, C. Adamo, J. Jaramillo, R. Gomperts, R. E. Stratmann, O. Yazyev, A. J. Austin, R. Cammi, C. Pomelli, J. W. Ochterski, R. L. Martin, K. Morokuma, V. G. Zakrzewski, G. A. Voth, P. Salvador, J. J. Dannenberg, S. Dapprich, A. D. Daniels, O. Farkas, J. B. Foresman, J. V. Ortiz, J. Cioslowski, D. J. Fox, *Gaussian 09* (Revision E.01), Gaussian, Inc., Wallingford CT, **2013**.
[32] A. D. Becke, *J. Chem. Phys.* **1993**, *98*, 5648–5652.
[33] Chemcraft, version 1.8, 2014: http://www.chemcraftprog.com.

Manuscript received: March 4, 2021
Revised manuscript received: April 15, 2021
Accepted manuscript online: April 22, 2021

FULL PAPERS

A series of 2-hydroxyphenyl-1H-benzo[d]imidazols bearing readily oxidizable 2,6-di-*tert*-butyl-phenol substituents and bis-chelate Cu(II) complexes based on these ligands were synthesized. Under oxidation both the ligands and Cu(II) complexes form stable phenoxyl-type radicals. As shown, no exchange interaction exists between unpaired electrons located on metal and oxygen centers in the Cu(II) complexes.

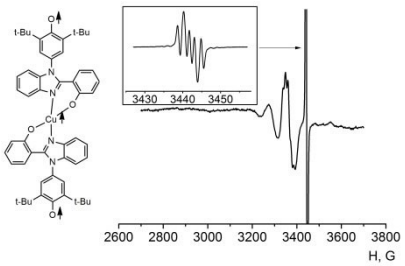

Prof. Dr. E. P. Ivakhnenko, P. A. Knyazev, Y. G. Vitkovskaya, L. D. Popov, Dr. K. A. Lyssenko, Dr. O. P. Demidov, Dr. A. G. Starikov, G. S. Borodkin, Prof. Dr. V. I. Minkin*